Eur Biophys J (2012) 41:991–1001
DOI 10.1007/s00249-012-0862-0

ORIGINAL PAPER

EBSA
Biophysics in Europe

Thermodynamics of strongly allosteric inhibition: a model study of HIV-1 protease

S. Kimura · R. A. Broglia · G. Tiana

Received: 5 June 2012 / Revised: 4 September 2012 / Accepted: 7 September 2012 / Published online: 5 October 2012
© European Biophysical Societies' Association 2012

Abstract Protein inhibitors that shift the thermodynamic equilibrium towards a denatured state escape, in general, the straightforward framework of competitive or allosteric inhibitors. The equilibrium properties of peptides which compete with the folding, or more precisely destabilize the native state, of the human immunodeficiency virus (HIV)-1 protease monomer are studied within a structure-based model. The effect of peptides that disrupt the hydrophobic core of the protein can still be summarized in terms of an inhibition constant, which depends on the thermal stability of the protein. The state of the protein denatured by such a peptide is more structured than its intrinsic denatured state, but displays the same degree of compactness. Peptides that target less buried regions of the protein are less efficient and display a more complex thermodynamics that cannot be captured in a simple way.

Keywords Protein folding inhibition · Monte Carlo sampling · Computational models · Inhibition constant

Electronic supplementary material The online version of this article (doi:10.1007/s00249-012-0862-0) contains supplementary material, which is available to authorized users.

S. Kimura · R. A. Broglia · G. Tiana (✉)
Department of Physics, University of Milano,
via Celoria 16, 20133 Milan, Italy
e-mail: tiana@mi.infn.it

S. Kimura · R. A. Broglia · G. Tiana
INFN, via Celoria 16, 20133 Milan, Italy

R. A. Broglia
The Niels Bohr Institute, Bledgamsvej 16,
2100 Copenhagen, Denmark

Introduction

The biophysical understanding of functional inhibition caused by the binding of a ligand to a semirigid protein is in general good, lying at the basis of the classical theory of inhibition (Segel 1993). By semirigid we mean that the target, although displaying some conformational freedom, can be pictured as populating one, or a few, thermodynamic states characterized by well-defined conformations (e.g., the native state of the protein, bound or unbound to the ligand). In this way, one can develop a formal theory of inhibition, including allosteric inhibition, in which the conformational thermodynamics is summarized by one (or a few) dissociation constants and whose main ingredients are the binding enthalpy of the ligand and the associated entropic loss (Finkelstein and Janin 1989).

Recently, light was shed on more radical inhibition mechanisms, involving molecules which cause major conformational changes in the target, and eventually the disruption of its active site. Examples of this phenomenon include dimerization inhibitors (Blasko et al. 2002; Zutshi and Chmielewski 2000) and folding inhibitors (Broglia et al. 2006, 2008; Pincus 1992). In all these cases the ligand affects the conformational properties of the target protein, shifting its thermodynamic equilibrium towards states in which the active site is not formed, resulting in a nonactive enzyme. This can, arguably, be viewed as an extreme case of allosteric inhibition. However, while in standard allosteric inhibition the target protein can usually move between a few well-defined conformations (Monod et al. 1965), in the present case the system can display a richer and, consequently, much more complicated thermodynamics.

A natural question that arises within this context is whether one can use the standard armory of theoretical

tools of protein inhibition to describe such nonstandard inhibition phenomena. In an attempt to answer this question, we present in what follows the results of a computational study of the aspartic protease of the HIV-1 virus. This enzyme is an important target of standard treatment against acquired immunodeficiency syndrome (AIDS). A peptide with the same sequence as segment 83–92 of the protease has been suggested (Broglia et al. 2005, 2006) to disrupt the hydrophobic core (13I, 15I, 33L, 64I, 84I, 85I), preventing the correct folding of the monomer which builds up the native dimer, thus making it inactive. The target of this peptide is the complementary segment of the protein that, in the native state, is in contact with segment 83–93, i.e., segment 24–34.

The HIV-1 protease (HIV-1-PR) is described with an implicit-solvent atomic model interacting through a structure-based potential (Go 1983). This approach consistently lightens the computational cost of carrying out thorough thermodynamic sampling of such a large system while still giving a correct description of the thermodynamics of the protein. In fact, structure-based potentials have been shown to account for several observables of proteins, such as the calorimetric properties (Shimada et al. 2001; Whitford et al. 2009), the structure of the transition state (Clementi et al. 2000; Lam et al. 2007; Sutto et al. 2006), the sequence of events along folding pathways (Shimada and Shakhnovich 2002), and the binding of monomers into oligomers (Levy et al. 2005). Although structure-based potentials were originally developed to describe systems in which only the experimental protein conformation displays favorable interactions, they have been successfully expanded to deal with more complex systems; For example, aggregation of SH3 (Ding et al. 2002) and superoxide dismutase has been described by including in the native-oriented potential a domain-swapping (non-native) term (Khare et al. 2005). In the present work, we follow a similar strategy, assuming that peptides interact with the protein exactly in the same way as the corresponding segments of the protein do.

Previous works on the protease were carried out with reduced models, accounting only for the C_α atom of each amino acid (Broglia et al. 2005; Cecconi et al. 2001; Potestio et al. 2009; Tozzini et al. 2007). Although providing an overall qualitatively correct picture of the dynamics of the protein, these models grossly misrepresent the quantitative aspects of its thermodynamics. The reason for this is that, in the C_α model, the degrees of freedom of the protein are oversimplified. Consequently the calculated value of the system's entropy and thus of the temperature are wrong. On the other hand, all-atom models with a structure-based potential provide a good approximation for the entropy of the system, resulting in sensible estimates of a number of thermodynamic quantities, at least in terms of orders of magnitude.

Folding inhibition represents a novel and potentially powerful way to inhibit deleterious proteins (see, e.g., Broglia et al. 2008 and references therein). Making use of a suitable computational model, we show that one should be careful in using the standard enzymatic theoretical framework, for example, the inhibition constant, to interpret folding inhibition data.

Results

Monte Carlo samplings of the conformational space of the protease monomer allow calculation of the equilibrium properties of the protease both alone and complexed with peptides. The specific heat of the protease monomer alone is displayed in the left panel of Fig. 1. The temperature in the calculations was adjusted in such a way that the folding temperature of the model coincides with the experimental one of 49 °C (Sayer et al. 2008). The protein displays a weakly cooperative transition between the native and a denatured state. In fact, the ratio between calorimetric and van't Hoff enthalpy is $\alpha = 2.6$, while it should be 1 for a pure two-state system and its average 1.05 for small single-domain proteins (Privalov and Khechinashvili 1974). This lack of cooperativity in the folding transition of the monomeric protease is not unexpected, since the protein evolved as a dimer. The probability p_D that the protein is in its denatured state, defined as the set of conformations displaying root-mean-square diameter (RMSD) larger than 7 Å (cf. right panel of Fig. 1), is shown in the top panel of Fig. 2. Within the model, we interpret p_D as an indicator of the functional activity of the protein, assuming that, if the monomer is in its denatured state, the HIV-1 protease is not biologically active (Noel et al. 2009).

Similar simulations have been carried out for a system built out of the monomeric protease and the peptide corresponding to segment 83–92 of the protease, and two other peptides, namely that corresponding to segment 24–34, which has also been suggested as a possible folding inhibitor of the protease (Broglia et al. 2005), and peptide 4–13, as a negative control peptide, in a cubic box of volume 10^3 nm^3 (see "Materials and methods"). The length of the simulations is adjusted such that it provides a sensible approximation to the equilibrium situation [Fig. S1 in the Electronic Supplementary Material (ESM)]. The presence of each of the peptides does not change the bimodal shape of the RMSD distribution (Fig. S2 in ESM), but results in a decrease of α to 1.8, that is, in an increase of the two-state character of the folding transition. The effect of the peptides on the probability p_D is also displayed in the top panel of Fig. 2. At about room temperature the

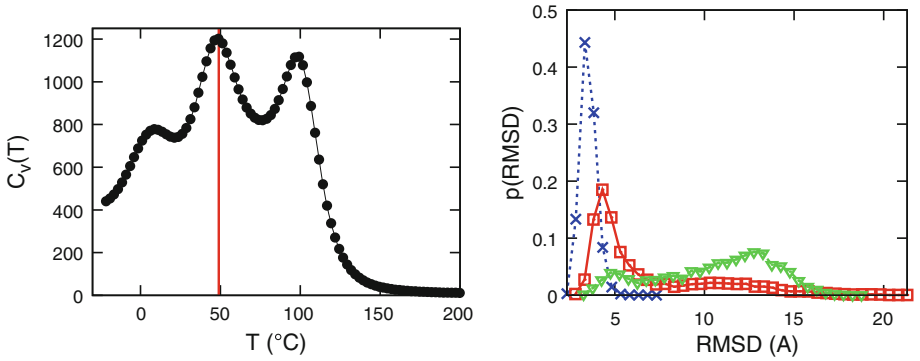

Fig. 1 (*Left panel*) The specific heat of the protease monomer obtained from Monte Carlo simulations. The temperature scale of the model was adjusted so that the folding temperature of the model coincides with the experimental one ($T_f = 49$ °C; Sayer et al. 2008), as marked by the *vertical red solid line*. The high-temperature peak ($T \approx 100$ °C) marks the coil–globule transition. (*Right panel*) The probability distribution of the RMSD with respect to the native conformation at $T = 44$ °C (*solid red curve*), $T = 3.6$ °C (*dotted blue curve*), and $T = 69$ °C (*green triangles*), respectively

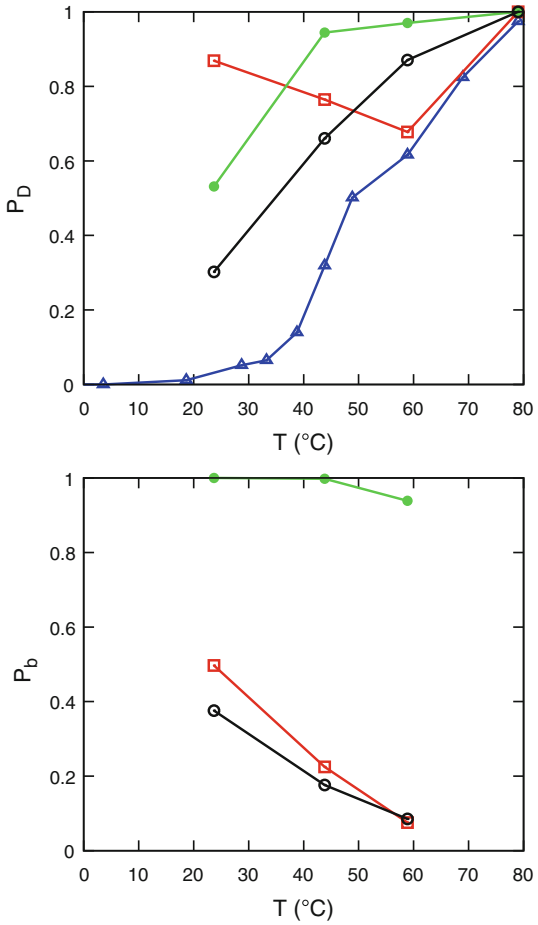

Fig. 2 (*Top panel*) Probability p_D that the HIV-1 protease monomer is in its denatured state as a function of temperature for the monomer alone (*blue triangles*) and complexed with peptide 83–92 (*red open squares*), 24–34 (*green filled circles*), and 4–13 (*black open circles*). (*Bottom panel*) Probability that the peptide is bound to the protein

inhibitory effect of peptide 83–92 is very marked, followed by that of peptide 24–34 and of peptide 4–13. Increasing the temperature, all the curves converge to large values of p_D because the denatured state of the protein is stabilized by its larger entropy with respect to the native state, thus reducing the inhibitory importance of the peptides. Moreover, p_D is increasing with respect to temperature in the case of peptides 24–34 and 4–13, while it is nonmonotonic (and slightly decreasing at biological temperature as compared with room temperature) for peptide 83–92, indicating that the entropy associated with the state denatured by this peptide is smaller than that associated with the other two peptides.

Structural properties of peptide-denatured state

The degree of compactness of the denatured state stabilized by the three peptides does not change significantly ($\lesssim 10\,\%$) with respect to that of the intrinsic denatured state of the protease (Fig. S3 in ESM). On the other hand, the corresponding denatured state results particularly structured; for example, the state of the protein denatured by peptide 83–92 at $T = 24$ °C (Fig. S4 in the ESM) displays the three native β-hairpins (10–19, 43–58, and 60–77) partially formed and several native and nonnative contacts between segment 20–40 and 70–95. From the structural point of view, it displays interesting similarities with the chemically denatured state, as studied experimentally by nuclear magnetic resonance (NMR) techniques; For example, secondary chemical shifts of the protease in 6 M guanidine indicate that residues 43, 44, 53, 55, 56 (corresponding to the second hairpin in the native conformation) and 66, 69 (corresponding to the third hairpin) display large beta propensities (Bhavesh et al. 2001). Moreover, residues 16, 18, 48, and 50 display high ^{15}N transverse relaxation rates, indicating constrained motion of that part of the chain (Bhavesh et al. 2003).

The above calculations also provide the probability p_b that a peptide is bound to its target in the monomer,

operatively defined as the probability that any atom of the peptide displays an attractive interaction with the monomer. The values of p_b for the three peptides are displayed in the lower panel of Fig. 2 as a function of temperature. At variance with what usually happens in conventional protein inhibition, the binding probability p_b behaves, as a function of temperature, very differently from the way the probability p_D that the protein is inactive behaves. In other words, binding is not related to inhibition in a straightforward way.

Thermodynamics of peptide-denatured state

The complex impact of the peptides on the equilibrium conformation of the HIV-1-PR monomer can be investigated by plotting the free energy of the monomer incubated with the corresponding peptides as a function of the overall RMSD of the protein and of the distance between the peptide and its target segment in the monomer (see "Materials and methods"). An example of such free energies calculated at room temperature is shown in Fig. 3, in comparison with the free energy of the monomer alone. The binding of peptide 83–93 to the protease results in a shift of the native state to a denatured state, displaying RMSD $\approx$ 10 Å, that is an ensemble of conformations which, on average, are more structured than the metastable denatured state in absence of the peptide. This is in keeping with the fact that the monomer–(83–92) complex displays native-like structure involving the exogenous peptide 83–92 and the segment 24–34 of the monomer. Peptide 24–34 displays, on the other hand, two free-energy minima for the bound state, indicating that the peptide also binds when the monomer is folded.

Since the binding of segment 24–34 to segment 83–92 is critical for the folding of the protease monomer (Broglia et al. 2005; Cecconi et al. 2001), it is of interest to map out the dependence of the free energy on the RMSD of the whole protein and of the structure built out of segments 24–34 and 83–92. The results, calculated at room temperature $T = 24$ °C, are displayed in Fig. 4. In the case of the monomer by itself, aside from the native minimum, the system populates states where segments 24–34 and 83–92 are native-like but the protein is overall unfolded, as well as states where neither this substructure nor the whole protein are structured (see also the free energy at the folding temperature in Fig. S5 of the ESM). The picture changes in presence of peptide 83–92, which causes a broadening of the free-energy minima and the population of several denatured states, including one where the protein is only slightly denatured but the 24–34/83–92 structure is not formed. Peptide 24–34 induces the stabilization of a native-like state where the region 24–34/83–92 is distorted, while peptide 4–13 has little effect on the stability of the native state, although it populates states which are slightly denatured and in which the region 24–34/83–93 is nonnative.

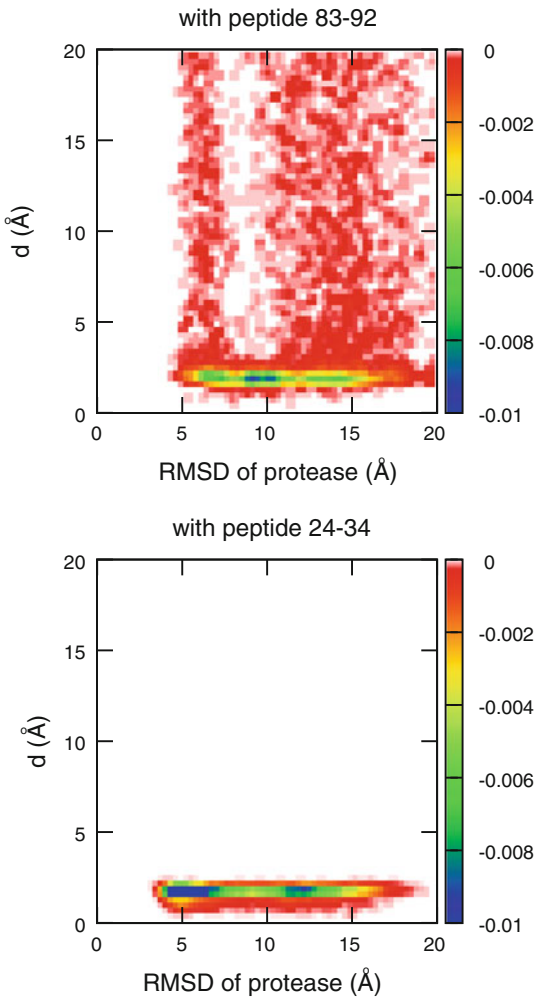

Fig. 3 Free energy (kJ/mol) of the monomer incubated with peptide 83–93 and 24–34 as a function of the overall RMSD and of the distance between the peptide and the monomer at room temperature $T = 24$ °C

A thermodynamic model for folding inhibition

The computational results obtained above can be interpreted within a simple thermodynamic scheme. The simulations indicate that, in all cases, the presence of the peptides does not invalidate the two-state behavior (native/denatured) of the protein (cf. Fig. S2 of the ESM). Moreover, the short-range character of the interactions allows the conformational space to be divided sharply into a subspace where the peptide is bound to its complementary segment of the protein, and one where it is not. Consequently one can define four states and assign them equilibrium probabilities such that

$$p_{Nb} + p_{Db} + p_{Nu} + p_{Du} = 1, \quad (1)$$

where the subscripts "N" and "D" indicate the native and the denatured states of the monomer, while the subscripts "b" and "u" indicate the bound and unbound states of the

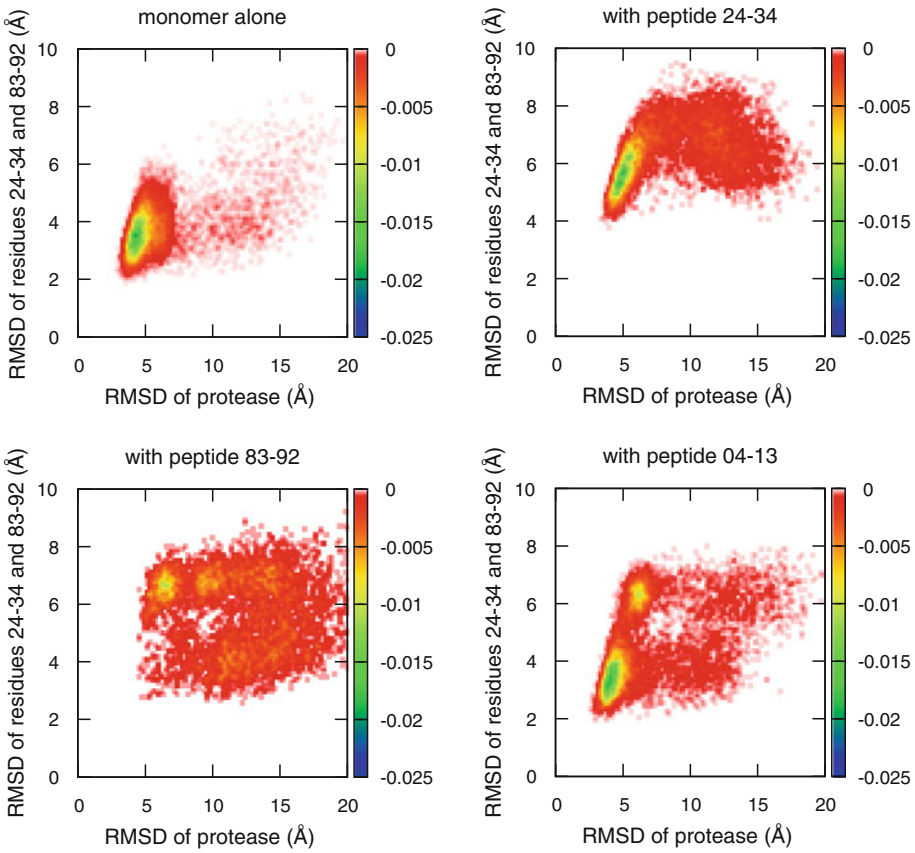

Fig. 4 Free energy (kJ/mol) of the HIV-1 protease monomer at $T = 24$ °C calculated from the results of Monte Carlo simulations for the monomer alone (*upper left panel*) and the monomer incubated with peptide 83–92 (*lower left panel*), as a function of the overall RMSD of the protein and of the RMSD associated with segments 83–92 and 24–34 of the monomer. The corresponding results obtained from the incubation of the monomer with peptides 24–34 and 4–13 are shown in the *panels of the right column*

peptide, respectively. A sketch of this thermodynamic model is reported in Fig. 5. Each of the probabilities satisfies, at equilibrium, Boltzmann statistics, that is, $p = \exp(-\Delta F/RT)/Z$, where ΔF is the free energy of the state in question defined with respect to a given reference state. Choosing for this, at each temperature, the state Nu, that is, the state in which the peptide is unbound (thus $\Delta F_{\mathrm{Nu}} = 0$), the free energies of the other states can be written as

$$\Delta F_{\mathrm{Db}} = \Delta F_{\mathrm{unfold}} + E_{\mathrm{pp}} + TS_{\mathrm{p}} + TS_{\mathrm{rt}}(\varrho), \tag{2a}$$

$$\Delta F_{\mathrm{Nb}} = E'_{\mathrm{pp}} + TS'_{\mathrm{p}} + TS_{\mathrm{rt}}(\varrho), \tag{2b}$$

$$\Delta F_{\mathrm{Du}} = \Delta F^{0}_{\mathrm{unfold}}, \tag{2c}$$

where $\Delta F^{0}_{\mathrm{unfold}} = F_{\mathrm{D}} - F_{\mathrm{N}}$ is the denaturing free energy of the monomer by itself, while $\Delta F_{\mathrm{unfold}} = F_{\mathrm{D}'} - F_{\mathrm{N}}$ is the unfolding free energy associated with the denatured state D′ (conformation inside dashed curve in Fig. 5a) in which the peptide is complexed, as a rule in terms of locally native-like binding, with the denatured monomer.

The quantity $E_{\mathrm{pp}}(E'_{\mathrm{pp}})$ is the interaction energy between peptide and the denatured (native) protein. In keeping with the fact that the exogenous peptide inhibits folding by substituting one of the two complementary segments of the protein in their native state, E_{pp} is likely to be close to the corresponding interaction energy value. The quantity $S_{\mathrm{p}}(S'_{\mathrm{p}})$ represents the entropic loss associated with the internal degrees of freedom of the peptide binding the denatured (native) state, while S_{rt} is the entropic loss associated with the roto-translational motion of the peptide upon binding. This is the only quantity entering the expressions introduced in (2a–2c) which depends on the concentration ρ of the peptide (Finkelstein and Janin 1989).

Denaturation by peptide 83–92

In the case of peptide 83–93, the probability that the monomer–peptide system is in the state Nb in which the peptide is bound and the protein is in the native state is quite negligible (Fig. 3; $p_{\mathrm{Nb}} \approx 10^{-4}$). In keeping with this (expected) result of the simulations, one can thus calculate ΔF_{Db} from the ratio between the Boltzmann probabilities

$$p_{\mathrm{Nu}} = \frac{1}{\exp\left[-\frac{\Delta F_{\mathrm{Db}}}{RT}\right] + \exp\left[-\frac{\Delta F^{0}_{\mathrm{unfold}}}{RT}\right] + 1},$$
$$p_{\mathrm{Db}} = \frac{\exp\left[-\frac{\Delta F_{\mathrm{Db}}}{RT}\right]}{\exp\left[-\frac{\Delta F_{\mathrm{Db}}}{RT}\right] + \exp\left[-\frac{\Delta F^{0}_{\mathrm{unfold}}}{RT}\right] + 1}, \tag{3}$$

obtaining

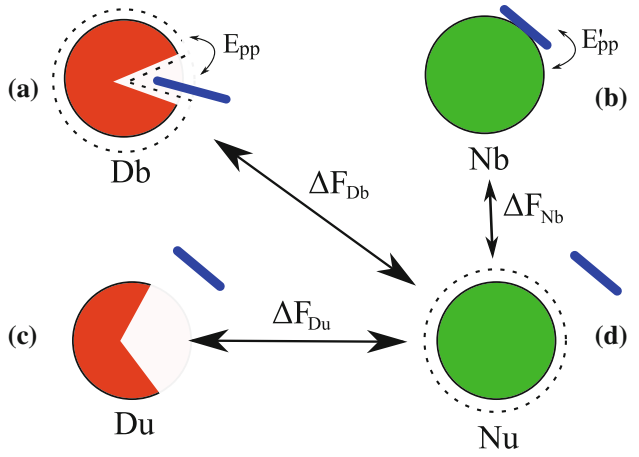

Fig. 5 A sketch of the thermodynamic model. *Green circles* indicate the folded protein, *red broken circles* indicate the denatured protein, and the *blue symbol* indicates the peptide. **a** Db: the state in which the protease monomer is denatured due to its binding to the peptide; **b** Nb: the state in which the protease monomer is folded, the peptide being bound to its surface; **c** Du: the state in which the protease monomer is in its intrinsic denatured state, the peptide being unbound [noting that this state is different from that appearing in **a**, which is surrounded by a *dashed curve* for easy reference, see also text after Eq. (2a–2c) as well as the caption to Fig. 6]; **d** Nu: the state in which the protein is in the native state and the peptide is unbound (this being the reference state; the native conformation of the monomer is encircled by a *dashed curve* for easy reference). In **a** and **b** the peptide–protein interaction is also indicated

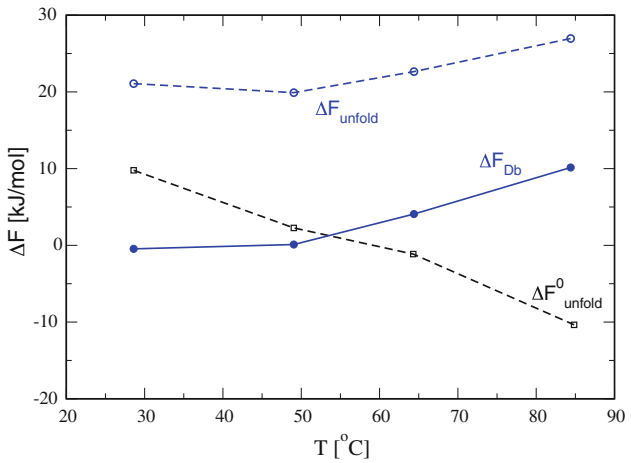

Fig. 6 The variety of free energies associated with the inhibition of the HIV-1 protease monomer by peptide 83–92. *Filled circles* indicate the free energy ΔF_{Db} of the denatured state bound to the peptide, with respect to the native, unbound state [see Fig. 5a, d, and Eq. (2a)]. *Empty circles* indicate a component of this free energy ($\Delta F_{\mathrm{unfold}}$), namely the unfolding free energy associated with the denatured state D′ (in which the peptide is complexed with the monomer) without taking into account either the interaction with the peptide or the contributions associated with the peptide entropy (see Fig. 5a, d, conformations inside *dashed curves*), while *empty squares* indicate the unfolding free energy ($\Delta F^{0}_{\mathrm{unfold}}$) of the isolated free protein

$$\Delta F_{\mathrm{Db}} = -RT \log \frac{p_{\mathrm{Db}}}{p_{\mathrm{Nu}}} = -RT \log \frac{p_{\mathrm{b}}}{p_{\mathrm{N}}}. \tag{4}$$

In the above equation use was made of the fact that, if the state Nb can be neglected, the probability associated with the state Db is equal to the overall probability p_{b} that the peptide is bound. Similarly, the probability of the system being in the state Nu becomes equal to the overall probability p_{N} that the protein is folded. This general result is rather useful because the quantities p_{b} and p_{N} can usually be obtained experimentally. The calculated values of ΔF_{Db} are displayed in Fig. 6. Deeper understanding of the corresponding results can be obtained by further splitting the free energy ΔF_{Db} into its components, following Eq. (2a–2c).

The value of S_{rt} is obtained by the analytical treatment described in Finkelstein and Janin (1989) as

$$S_{\mathrm{rt}} = R \log \frac{1}{\rho \delta x^3} - \frac{R}{8\pi^2} \log \delta\alpha^3, \tag{5}$$

where the first term accounts for the translational entropy, $\rho = 10^{-6}$ Å^{-3} is the peptide concentration used in the simulation, while $\delta x^3 = 8$ Å^3 is the volume defined by the square-well interaction used in the model. The second term in Eq. (5) accounts for the rotational entropy, $\delta\alpha^3 = 8\delta x^3/d^3$ corresponding to the angular freedom of the bound peptide, where $d^3 = 7.7 \times 10^3$ Å^3 is the volume enclosed by the contact interface between the peptide and the protein. With the above parameters one obtains $S_{\mathrm{rt}} = 7.5R$.

The values of E_{pp} and S_{p} cannot be obtained from the present simulation, but are extracted from a sampling of peptide 83–93 incubated with a peptide with the same sequence as its target, i.e., segment 24–34 of the protein. In this case, peptide 83–92 is expected to display, upon docking with the target, the same binding energy E_{pp} and entropic loss S_{p} as the corresponding event in which the peptide binds to the protease monomer. The main difference between this event and the peptide–peptide case under discussion is that the binding of 83–92 does not have to pay the free-energy cost associated with monomer unfolding, except for the part associated with structuring of region 24–34. Thus, to determine the binding energy E_{pp} and the entropic loss S_{p} associated with only the structuring of peptide 83–92, we carried out two simulations: (A) binding at equilibrium of peptides 83–92 and 24–34, and (B) binding of peptide 83–93 to a peptide with the same sequence as peptide 24–34, but artificially forced to rigidly occupy its native conformation (i.e., the conformation that the corresponding segment of the protein monomer displays in the experimental native state). Both binding probabilities (Fig. S6 in the ESM) are expected to satisfy

$$p_{\mathrm{b}}^{\mathrm{peptide}} = \frac{\exp\left[-\frac{E_{\mathrm{pp}}+TS_{\mathrm{p}}+TS_{\mathrm{rt}}}{RT}\right]}{1+\exp\left[-\frac{E_{\mathrm{pp}}+TS_{\mathrm{p}}+TS_{\mathrm{rt}}}{RT}\right]}, \quad (6)$$

where S_{p} is the entropy loss associated with the internal degrees of freedom of both peptides (simulation A) and of only peptide 83–92 (simulation B). A least-squares fit to the binding probability gives $E_{\mathrm{pp}} = -46.4$ kJ/mol and $S_{\mathrm{p}} = 3.9R$ for simulation A and $E_{\mathrm{pp}} = -53.1$ kJ/mol and $S_{\mathrm{p}} = 1.9R$ for simulation B. The numerical values needed in Eq. (2a–2c) are those resulting from simulation B. To use this strategy making use of experimental data, one faces the problem that only the binding probability corresponding to simulation A can be measured. However, the comparison of the two simulations suggests that the entropy loss per monomer is approximately constant (3.9/21 = 0.185 if both peptides are free to move, 1.9/10 = 0.190 if only peptide 83–92 can move). Consequently, one can measure the binding probability of two peptides that are free to move, and extract the entropy associated with one of the two, from the ratio of their lengths.

Substituting into Eq. (2a–2c) the numerical values obtained above, one obtains

$$\Delta F_{\mathrm{unfold}} = \Delta F_{\mathrm{Db}} - E_{\mathrm{pp}} - TS_{\mathrm{p}} - TS_{\mathrm{rt}},$$

whose behavior as a function of temperature is displayed in Fig. 6 together with that of $\Delta F_{\mathrm{f}}^{0}$, calculated in absence of the peptide, that is, the monomer by itself. The value of $\Delta F_{\mathrm{unfold}}$ is positive at all temperatures, being larger than that of $\Delta F_{\mathrm{unfold}}^{0}$, indicating that the denatured state of the protein bound to the peptide is energetically different from the denatured state of the isolated protein. In particular, it is more unfavorable than that of the protein in isolation. Its weak dependence on temperature suggests that, at variance with typical denatured states, it is mainly stabilized energetically.

Summing up, unlike what happens in conventional inhibition, peptide 83–92 causes a consistent conformational change in the monomer, likely disfavoring the formation of the active native state, and for that it has to pay a consistent additional free-energy cost, which is, at temperature $T = 20$–40 °C, larger (by 5–10 kJ/mol) than the denaturing free energy of the protein.

Denaturation by peptides 24–34 and 4–13

In the case of peptide 24–34 the situation is more complicated, because the state Nb is no longer negligible, and the thermodynamics is controlled by all of the four states introduced above. Inverting the Boltzmann distributions and inserting the calculated probability of states Db and Nb, one can obtain the associated free energies, which are displayed in Fig. 7. The native state Nb of the protein with

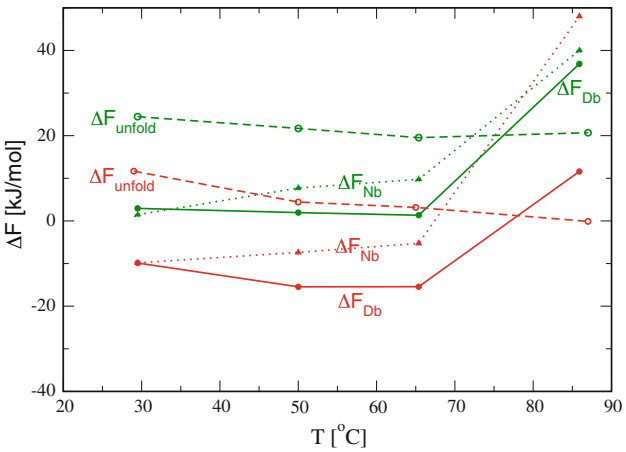

Fig. 7 Free energies associated with the inhibition of the HIV-1 protease monomer by peptides 24–34 (*red*) and 4–13 (*green*). *Filled circles* indicate the free energy ΔF_{Db} of the denatured state bound to the peptide, and *filled triangles* that (ΔF_{Nb}) of the native state bound to the peptide, both calculated with respect to the native, unbound state. *Empty circles* indicate the unfolding free energy $\Delta F_{\mathrm{unfold}}$, net of the interaction with the peptide (see also the caption to Fig. 6)

the peptide attached from outside displays a free energy that is slightly larger than, but anyway comparable to, the state Db denatured by the peptide. The component of the peptide-induced denaturing free energy $\Delta F_{\mathrm{unfold}}$ associated with the protein is very similar to the denaturing free energy $\Delta F_{\mathrm{unfold}}^{0}$ of the protein alone, suggesting that the state Db is thermodynamically similar to that in absence of any peptide.

Control peptide 4–13 destabilizes the native state of the protein by few kJ/mol (Fig. 7), displaying a $\Delta F_{\mathrm{unfold}}$ larger than $\Delta F_{\mathrm{unfold}}^{0}$, indicating an unfavorable (more native-like) denatured state.

Equilibrium constants

From the above calculations it is simple to generalize the simulations carried out at fixed concentration of peptides (10^{-6} Å^{-3}) to other concentrations. In fact, peptide concentration enters the free energies described by Eq. (2a–2c) only via the roto-translational entropy S_{rt}, whose dependence on concentration is given in Eq. (5). A consequence of this fact is that the probabilities associated with all states, including their sums $p_{\mathrm{b}} = p_{\mathrm{Db}} + p_{\mathrm{Nb}}$ and $p_{\mathrm{D}} = p_{\mathrm{Db}} + p_{\mathrm{Du}}$, display a sigmoidal shape (cf. Eq. S1 in the ESM) as in standard bimolecular binding, except for the fact that p_{D} converges to a nonzero value (i.e., p_{D} converges to a value obtained from the simulations of the protease in the absence of any peptide) as the density decreases to zero (cf. Fig. S7 in ESM).

An interesting issue concerning the concentration dependence of the above probabilities is whether it is possible to define some equilibrium constants to easily

estimate the range of concentrations for which inhibition takes place. The first difference from conventional inhibition is that, in general, binding and inhibition curves (i.e., the probabilities associated with the unbound and with the denatured state, respectively) are quite different from each other, so one does not expect to capture all the thermodynamics by a single equilibrium constant (see Fig. 2). The definition of a dissociation constant is straightforward, that is,

$$k_{\mathrm{D}} = \rho \frac{1 - p_{\mathrm{b}}}{p_{\mathrm{b}}} = \rho \exp\left[-\frac{\Delta F_{\mathrm{u}} - \Delta F_{\mathrm{b}}}{RT}\right]. \tag{7}$$

If one substitutes here Eq. (5) and the expressions of the free energy of the unbound state $\Delta F_{\mathrm{u}} = -RT \log[\exp(-\Delta F_{\mathrm{Nu}}/RT) + \exp(-\Delta F_{\mathrm{Du}}/RT)]$ and of the bound state $\Delta F_{\mathrm{b}} = -RT \log[\exp(-\Delta F_{\mathrm{Nb}}/RT) + \exp(-\Delta F_{\mathrm{Db}}/RT)]$, one obtains an expression which is independent of the concentration ρ. The temperature dependence of this constant is shown in the top panel of Fig. 8.

Similarly, one could define an inhibition constant k_{I} based on the probability that the protein is in the inactive denatured state D, that is,

$$k_{\mathrm{I}} = \rho \frac{1 - p_{\mathrm{D}}}{p_{\mathrm{D}}} = \rho \exp\left[-\frac{\Delta F_{\mathrm{N}} - \Delta F_{\mathrm{D}}}{RT}\right]. \tag{8}$$

The problem here is that, in general, k_{I} is not independent of ρ due to the nontrivial mix of concentration-dependent and concentration-independent terms in the free energies of Eq. (8) (cf. Eq. S3 in the Supplementary Material). Consequently, k_{I} is not appropriate for the purpose of estimating the inhibitory concentration of a peptide, except in the limit of large $\Delta F^0_{\mathrm{unfold}}$ or the absence of a populated Nb state, as in the case of peptide 83–93 at low temperature (cf. above). On the other hand, if the Nb state is populated, no meaningful definition of an equilibrium constant in terms of concentration is possible. If this is not the case, but still there is a populated Du state, one can define the constant

$$k_{\mathrm{I}} = \rho \frac{1 - p_{\mathrm{Db}}}{p_{\mathrm{Db}}} = \rho \frac{\exp\left[-\frac{\Delta F^0_{\mathrm{unfold}}}{RT}\right] + 1}{\exp[-S_{\mathrm{rt}}(\rho)] \exp\left[-\frac{\Delta F_{\mathrm{unfold}} + E_{\mathrm{pp}} + TS_{\mathrm{p}}}{RT}\right]}, \tag{9}$$

which provides a measure of the net effect of the peptide on the folding of the protein, which is concentration independent. Experimentally, Eq. (9) can be determined as $p_{\mathrm{Db}} = p_{\mathrm{D}} - p^0_{\mathrm{D}}$, where p^0_{D} is the probability associated with the denatured state of the protein in absence of any peptide. Of course, in the limit in which p^0_{D} is negligible, one obtains the simple behavior shown by peptide 83–92. The temperature dependence of k_{I} as defined in Eq. (9) for peptide 83–93 is displayed in the bottom panel of Fig. 8.

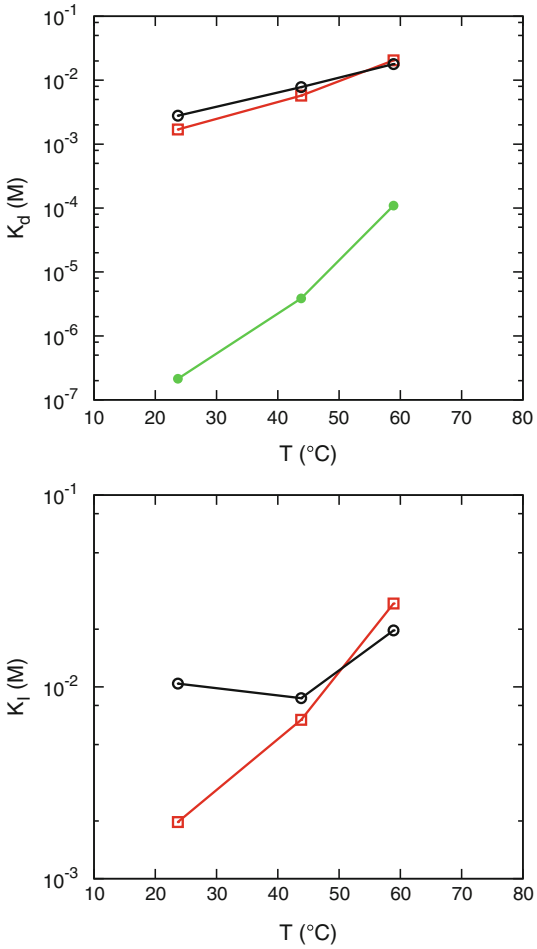

Fig. 8 (*Top panel*) The dissociation constant for the protein complexed with peptide 83–92 (*red open squares*), 24–34 (*green filled circles*), and 4–13 (*black open circles*). (*Bottom panel*) The inhibition constant for the protein complexed with peptide 83–92 (*red open squares*) and 4–13 (*black open circles*)

An important feature of the inhibition constant (9) is that, unlike those involved in conventional inhibition, it depends strongly on the stability $\Delta F^0_{\mathrm{unfold}}$ of the protein (cf. Eq. 9). This means that mutations in the protein that do not affect the binding site of the peptide but anyhow change the overall stability of the protein are able to modify the inhibition constant (9). The behavior of k_{I} for peptide 83–92 as a function of the stability of the protein in isolation is displayed in Fig. 9 (similarly, an estimate of the change in k_{I} upon modification of the peptide, causing a change $\Delta\varepsilon$ in the interaction energy E_{pp}, is shown in Fig. S8).

Inhibition of HIV-1-PR dimer

The above discussion on the inhibition constant k_{I} for the monomeric HIV-1 protease can be easily extended to

include the dimeric phase of the enzyme. Defining p_2 as the probability that the protein is in dimeric form and p_1 as the probability that is in the monomeric form, then $p_2 + p_1 = 1$. Thus, Eq. (1) can be extended to include the folded dimeric protein,

$$p_2 + p_1 \times (p_{\mathrm{Nu}} + p_{\mathrm{Du}} + p_{\mathrm{Db}}) = 1, \tag{10}$$

where we neglect the term p_{Nb}, considering only the case of the protein complexed with peptide 83–92. The dissociation constant between dimer and its monomer (k_{DP}; of notice that in this case D stands for dimer and P for protein monomer) is, by definition,

$$k_{\mathrm{DP}} = \rho_{\mathrm{E}} \exp\left[-\frac{\Delta F_1 - \Delta F_2}{RT}\right], \tag{11}$$

where ρ_{E} is the concentration of the enzyme and $\Delta F_1 = -RT \log[\exp(-\Delta F_{\mathrm{Du}}/RT) + \exp(-\Delta F_{\mathrm{Db}}/RT) + 1]$. The partition function of the system is

$$\begin{aligned} Z &= 1 + \exp\left[-\frac{\Delta F_2}{RT}\right] \exp\left[-\frac{\Delta F_1 - \Delta F_2}{RT}\right] \\ &= \exp\left[-\frac{\Delta F_2}{RT}\right]\left(1 + \frac{k_{\mathrm{DP}}}{\rho_{\mathrm{E}}}\right), \end{aligned} \tag{12}$$

and the probability of the monomeric form is then

$$p_1 = \frac{\exp\left[-\frac{\Delta F_1}{RT}\right]}{Z} = \frac{k_{\mathrm{DP}}}{\rho_{\mathrm{E}} + k_{\mathrm{DP}}}. \tag{13}$$

Modifying Eq. (9), the inhibition constant associated with the peptide can then be rewritten as

$$\begin{aligned} k_{\mathrm{I}} &= \rho \frac{1 - p_1 p_{\mathrm{Db}}}{p_1 p_{\mathrm{Db}}} \\ &= \frac{\frac{\rho_{\mathrm{E}}}{k_{\mathrm{DP}}} + \exp\left[-\frac{\Delta F^0_{\mathrm{unfold}}}{RT}\right] + 1}{\varrho^{-1} \exp[-S_{\mathrm{rt}}(\rho)/R] \exp\left[-\frac{\Delta F_{\mathrm{unfold}} + E_{\mathrm{pp}} + TS_{\mathrm{p}}}{RT}\right]}, \end{aligned} \tag{14}$$

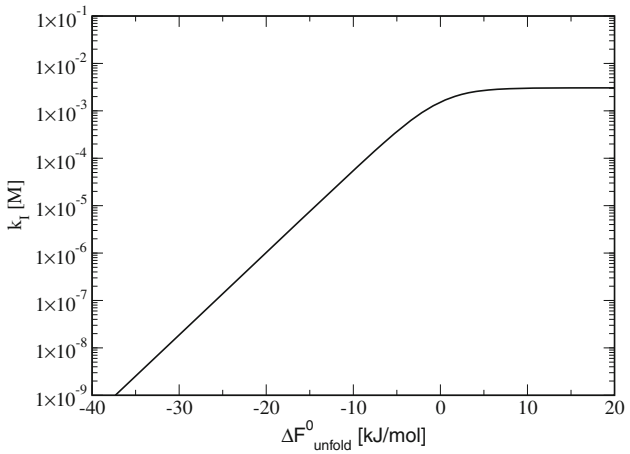

Fig. 9 Inhibition constant of peptide 83–92 as a function of the thermal stability of the protein

which is independent of the concentration ρ of peptide because it cancels out in the denominator of the above equation. On the other hand, k_{I} depends on the protein concentration, a quantity which can shift the monomer–dimer equilibrium value. Such a dependence is shown in Fig. 10 as a function of the dissociation constant k_{DP}.

Materials and methods

The protein is described in terms of all its heavy atoms, which interact through a potential of the form

$$\begin{aligned} U = &-\frac{1}{2}\sum_{i<j}\theta\left(1.05\left|r_i^{\mathrm{N}} - r_j^{\mathrm{N}}\right| - |r_i - r_j|\right)\theta\left(0.35\,\mathrm{nm} - \left|r_i^{\mathrm{N}} - r_j^{\mathrm{N}}\right|\right) \\ &-\frac{1}{2}\sum_{i<j}\theta\left(2.1\left|r_i^{\mathrm{N}} - r_j^{\mathrm{N}}\right| - |r_i - r_j|\right)\theta\left(0.35\,\mathrm{nm} - \left|r_i^{\mathrm{N}} - r_j^{\mathrm{N}}\right|\right) \\ &+\left[\theta\left(|r_i - r_j| - 0.9\left|r_i^{\mathrm{N}} - r_j^{\mathrm{N}}\right|\right)\right]^{-1}\sum_{i<j}\theta\left(0.35\,\mathrm{nm} - \left|r_i^{\mathrm{N}} - r_j^{\mathrm{N}}\right|\right) \\ &+\sum_{i<j}\left[\theta\left(|r_i - r_j| - 0.2\,\mathrm{nm}\right)\right]^{-1} + 0.5\sum_i\left(1 + \cos[\varphi_i - \varphi_{\mathrm{Ni}}]\right) \\ &+0.25\sum_i\left(1 + \cos[3(\varphi_i - \varphi_{\mathrm{Ni}})]\right), \end{aligned}$$

where r_i is the coordinate of the i-th atom, r_i^{N} is its coordinate in the native conformation, the function θ is a step function which takes the value 1 if its argument is positive and zero otherwise, φ_i is the dihedral associated with the ith Ramachandran dihedral, and φ_{Ni} is its value in the native conformation. Thus, the two-body term defined by the first two sums introduces a double square well which roughly approximates a Lennard–Jones potential and whose minimum lies close to the native distance of each pair. The third sum defines a hard-core repulsion for native

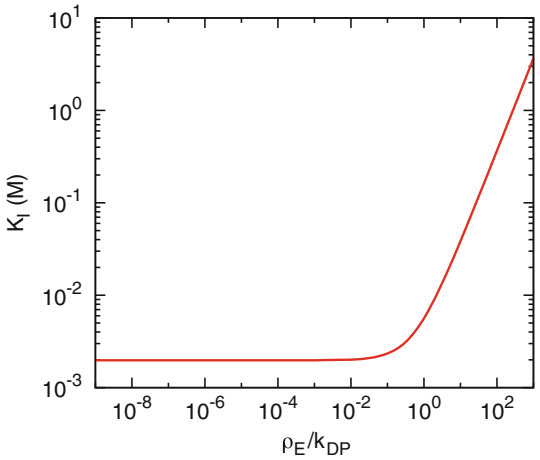

Fig. 10 Inhibition constant for the HIV-1-PR dimer incubated with peptide 83–92 at $T = 24$ °C as a function of the ratio $\rho_{\mathrm{E}}/k_{\mathrm{DP}}$ between the concentration of protein and the monomer–dimer dissociation constant k_{DP}

pairs at a distance slightly shorter than the native distance, and the fourth term defines a global hard-core repulsion between any pair of atoms at 0.2 nm (which can overrule the previous one). The system is constrained in a cubic box of side 10 nm.

The atoms belonging to the peptide corresponding to segment $i-j$ of the protein interact in a way that is identical to that of the corresponding atoms in the protein.

The sidechains can move rigidly among the rotamers defined in Lovell et al. (2000).

The native conformation of the protease is taken from structure 1BVG of the Protein Data Bank. Native contacts are defined for those pairs of heavy atoms which are closer than 0.35 nm in such a native conformation.

The equilibrium sampling is carried out through a Monte Carlo scheme at fixed temperature, including pivot moves, multiple pivot moves (Shimada et al. 2001), movement of the sidechains among their rotamers, and displacement of the center of mass.

Simulations with the peptide are carried out by inserting the peptide into the box at a random position, detached from the protein, and moving it according to the same Monte Carlo scheme as used for the protein.

The specific heat is calculated by means of the multiple histogram method (Ferrenberg and Swendsen 1989). First, the average energy and the associated standard deviation are obtained as a function of temperature, and then the standard deviation is used to calculate the specific heat by making use of the fluctuation–dissipation theorem.

The free-energy landscapes are calculated by simply inverting the Boltzmann distribution.

Discussion

The inactivation of an enzyme obtained by blocking its folding to the native state is qualitatively different from conventional competitive or allosteric inhibition. The inactive form is an entropy-rich state composed of denatured conformations. The binding of peptide 83–92, to which we refer in what follows, is incompatible with the formation of the hydrophobic core of the native monomer. The result is a monomeric denatured state which is however more structured than the intrinsic denatured state of the unbound monomer. In fact, the denatured state induced by the peptide displays a free energy which is larger by several RT than that of the intrinsic denatured state.

At both low temperature, where inhibition involves only two states, and higher temperature, where also the intrinsically denatured state is populated, it is possible to define an inhibition constant k_I which indicates the inhibitory concentration of the peptide. At variance with conventional inhibition, in the case of folding inhibitors the value of k_I is in general different from the binding constant k_B. However, the most peculiar feature of this kind of strongly allosteric folding inhibitors is that the value of k_I depends on the intrinsic stability of the protein, that is, on $\Delta F^0_{\text{unfold}}$. Although we do not expect that the simple structure-based model employed in the present simulations can provide a quantitatively accurate inhibition constant, it contains the physical ingredients needed to reveal the qualitative behavior of k_I as a function of $\Delta F^0_{\text{unfold}}$ shown in Fig. 9. The resulting picture suggests that the ability of the peptide to inhibit the protein can be environment dependent, as different cellular environments can modify the intrinsic stability of the protein. Moreover, a strategy that the virus could follow to develop pharmacological resistance against the peptide is to stabilize its native state, mutating sites which can be far away the target region. These are all problems which should be dealt with when attempting to turn the peptide into an antiviral drug.

The model shows that, as the peptide binds to the interior of the denatured protein, it has to pay an additional energy cost compared with if it had to bind to the protein surface, namely the cost of denaturing the protein. This cost is somewhat larger than the full intrinsic denaturing free energy of the protein, because it refers to a different denatured state. At room temperature, the full denaturing free energy of monomer denaturation is 10 kJ/mol according to the model, which is comparable to the typical experimental values of monomeric variants of the protease [i.e., 5.1 kJ/mol for the Δ96–99 mutant at pH 6 in sodium phosphate buffer (Noel et al. 2009), but of course variable with mutation and with environmental conditions]. On the other hand, the free energy cost that the peptide pays to denature the protein is 16.4 kJ/mol, according to the model calculations. The reason is that the peptide stabilizes a denatured state that is more unlikely than the intrinsic denatured state of the protein because of its lower entropic content.

The monomeric HIV-1 protease reflects the state of the protein when embedded in the precursor (Chatterjee et al. 2005; Tang et al. 2008). After cleavage from the precursor, the protease dimerizes, something which further stabilizes the native state of the monomer. Thus, the inhibition constant of peptide 83–92 increases following the behavior described in Fig. 10. The dimerization constant of the protease varies consistently according to the specific sequence and the environmental conditions, ranging from picomolar (Todd et al. 1998) to micromolar (Xie et al. 1999). Consequently, also the effect of dimerization on the inhibition constant of the peptide varies accordingly.

The thermodynamics associated with binding of the other two peptides is more complex, and cannot be summarized into an inhibition constant. Peptide 24–34 can bind both the interior of the protein, preventing folding,

and the outside, which could also be of interest to prevent dimerization. The overall binding tendency to the protease is much larger than that of peptide 83–92, but with a smaller monomeric inhibitory effect.

Conclusions

The use of a simplified structure-based model allows exploration of the thermodynamics of HIV-1 protease complexed with folding inhibitor peptides, something that explicit-solvent computational models cannot do. The effect of peptides which compete with the formation of the hydrophobic core of the protein can be described effectively in terms of an inhibition constant which depends on the thermal stability of the protein, including its dimerized state. Peptides targeting other regions of the protease have a smaller inhibitory effect and a more complicated thermodynamics. Anyway, the denatured state stabilized by such peptides is different, and more structured, than the intrinsic denatured state of the protein.

References

Bhavesh NS, Panchal SC, Mittal R, Hosur RV (2001) NMR identification of local structural preferences in HIV-1 protease tethered heterodimer in 6 M guanidine hydrochloride. FEBS Lett 509:218–224

Bhavesh NS, Sinha R, Mohan PMK, Hosur RV (2003) NMR elucidation of early folding hierarchy in HIV-1 protease. J Biol Chem 278:19980–19985

Blasko E, Glaser CB, Devlin JJ et al (2002) Mechanistic studies with potent and selective inducible nitric-oxide synthase dimerization inhibitors. J Biol Chem 277:295–302. doi:10.1074/jbc.M105691200

Broglia RA, Tiana G, Sutto L et al (2005) Design of HIV-1-PR inhibitors that do not create resistance: blocking the folding of single monomers. Protein Sci 14:2668–2681. doi:10.1110/ps.051670905

Broglia RA, Provasi D, Vasile F et al (2006) A folding inhibitor of the HIV-1 protease. Proteins 62:928–933. doi:10.1002/prot.20849

Broglia RA, Levy Y, Tiana G (2008) HIV-1 protease folding and the design of drugs which do not create resistance. Curr Opin Struct Biol 18:60–66. doi:10.1016/j.sbi.2007.10.004

Cecconi F, Micheletti C, Carloni P, Maritan A (2001) Molecular dynamics studies on HIV-1 protease drug resistance and folding pathways. Proteins 43:365–372. doi:10.1002/prot.1049

Chatterjee A, Mridula P, Mishra RK et al (2005) Folding regulates autoprocessing of HIV-1 protease precursor. J Biol Chem 280:11369–11378. doi:10.1074/jbc.M412603200

Clementi C, Nymeyer H, Onuchic JN (2000) Topological and energetic factors: what determines the structural details of the transition state ensemble and en-route intermediates for protein folding? J Mol Biol 296:937–953

Ding F, Dokholyan NV, Buldyrev SV, Stanley HE, Shakhnovich EI (2002) Molecular dynamics simulation of the SH3 domain aggregation suggests a generic amyloidogenesis mechanism. J Mol Biol 324:851–857

Ferrenberg AM, Swendsen RH (1989) Optimized Monte Carlo data analysis. Phys Rev Lett 63:1195–1198

Finkelstein A, Janin J (1989) The price of lost freedom: entropy of bimolecular complex formation. Protein Eng 3:1–3

Go N (1983) Theoretical studies of protein folding. Annu Rev Biophys Bioeng 12:183–210. doi:10.1146/annurev.bb.12.060183.001151

Khare SD, Wilcox KC, Gong P, Dokholyan NV (2005) Sequence and structural determinants of Cu, Zn superoxide dismutase aggregation. Proteins 61:617–632. doi:10.1002/prot.20629

Lam AR, Borreguero JM, Ding F et al (2007) Parallel folding pathways in the SH3 domain protein. J Mol Biol 373:1348–1360. doi:10.1016/j.jmb.2007.08.032

Levy Y, Cho SS, Onuchic JN, Wolynes PG (2005) A survey of flexible protein binding mechanisms and their transition states using native topology based energy landscapes. J Mol Biol 346:1121–1145

Lovell SC, Word JM, Richardson JS, Richardson DC (2000) The penultimate rotamer library. Proteins 40:389–408

Monod J, Wyman J, Cjangeux JP (1965) On the nature of allosteric transitions: a plausible model. J Mol Biol 12:88–118

Noel AF, Bilsel O, Kundu A et al (2009) The folding free-energy surface of HIV-1 protease: insights into the thermodynamic basis for resistance to inhibitors. J Mol Biol 387:1002–1016. doi:10.1016/j.jmb.2008.12.061

Pincus MR (1992) Identification of structured peptide segments in folding proteins. Biopolymers 32:347–351. doi:10.1002/bip.360320409

Potestio R, Pontiggia F, Micheletti C (2009) Coarse-grained description of protein internal dynamics: an optimal strategy for decomposing proteins in rigid subunits. Biophys J 96:4993–5002. doi:10.1016/j.bpj.2009.03.051

Privalov PL, Khechinashvili NN (1974) A thermodynamic approach to the problem of stabilization of globular protein structure: a calorimetric study. J Mol Biol 86:665–684

Sayer JM, Liu F, Ishima R et al (2008) Effect of the active site D25N mutation on the structure, stability, and ligand binding of the mature HIV-1 protease. J Biol Chem 283:13459–13470. doi:10.1074/jbc.M708506200

Segel IH (1993) Enzyme kinetics: behavior and analysis of rapid equilibrium and steady-state enzyme systems. Wiley, London

Shimada J, Shakhnovich EI (2002) The ensemble folding kinetics of protein G from an all-atom Monte Carlo simulation. Proc Natl Acad Sci USA 99:11175–11180. doi:10.1073/pnas.162268099

Shimada J, Kussell EL, Shakhnovich EI (2001) The folding thermodynamics and kinetics of crambin using an all-atom Monte Carlo simulation. J Mol Biol 308:79–95. doi:10.1006/jmbi.2001.4586

Sutto L, Tiana G, Broglia RA (2006) Sequence of events in folding mechanism: beyond the Go model. Protein Sci 15:1638–1652

Tang C, Louis JM, Aniana A et al (2008) Visualizing transient events in amino-terminal autoprocessing of HIV-1 protease. Nature 455:693–696. doi:10.1038/nature07342

Todd MJ, Semo N, Freire E (1998) The structural stability of the HIV-1 protease. J Mol Biol 283:475–488. doi:10.1006/jmbi.1998.2090

Tozzini V, Trylska J, Chang C-E, McCammon JA (2007) Flap opening dynamics in HIV-1 protease explored with a coarse-grained model. J Struct Biol 157:606–615. doi:10.1016/j.jsb.2006.08.005

Whitford PC, Noel JK, Gosavi S et al (2009) An all-atom structure-based potential for proteins: bridging minimal models with all-atom empirical forcefields. Proteins 75:430–441. doi:10.1002/prot.22253

Xie D, Gulnik S, Gustchina E et al (1999) Drug resistance mutations can effect dimer stability of HIV-1 protease at neutral pH. Protein Sci 8:1702–1707

Zutshi R, Chmielewski J (2000) Targeting the dimerization interface for irreversible inhibition of HIV-1 protease. Bioorg Med Chem Lett 10:1901–1903